Spatial phosphoprotein profiling reveals a compartmentalized ERK switch governing neurite growth and retraction

16 authors, including:

Yingchun Wang
Institute of Genetics and Developmental Biology, Chinese Academy of Sciences
215 PUBLICATIONS   **5,806** CITATIONS

SEE PROFILE

Feng Yang
Southwest Jiaotong University
104 PUBLICATIONS   **3,187** CITATIONS

SEE PROFILE

Xiahe Huang
Institute of Genetics and Developmental Biology, Chinese Academy of Sciences
79 PUBLICATIONS   **2,600** CITATIONS

SEE PROFILE

Wang Wei
Institute of Genetics and Developmental Biology, Chinese Academy of Sciences
52 PUBLICATIONS   **4,016** CITATIONS

SEE PROFILE

SPATIAL PHOSPHOPROTEIN PROFILING REVEALS A COMPARTMENTALIZED ERK SWITCH GOVERNING NEURITE GROWTH AND RETRACTION

Yingchun Wang[1,3,¶], Feng Yang[2,¶], Yi Fu[3], Xiahe Huang[3], Wei Wang[1,3], Xinning Jiang[1], Marina A. Gritsenko[2], Rui Zhao[2], Matthew E. Monore[2], Olivier C. Pertz[1,4], Samuel O. Purvine[2], Daniel J. Orton[2], Jon M. Jacobs[2], David G. Camp II[2], Richard D. Smith[2], and Richard L. Klemke[1,*]

From Department of Pathology and Moores Cancer Center [1], University of California, San Diego, La Jolla, CA 92093.
Biological Sciences Division, Environmental Molecular Sciences Laboratory [2], Pacific Northwest National Laboratory, Richland, WA 99354.
Present address: Key Laboratory of Molecular and Developmental Biology [3], Institute of Genetics and Developmental Biology, Chinese Academy of Sciences, Beijing, 100101, China.
Present address: Institute of Biochemistry and Genetics, Department of Biomedicine [4], University of Basal, CH-4003 Basel, Switzerland.
Running Head: ERK Governs Neurite Dynamics
[¶] These authors contributed equally to this work.
Address correspondence to: Richard L. Klemke, Department of Pathology and Moores Cancer Center, University of California, San Diego, Basic Science Building 1040, 9500 Gilman Drive, MC 0612, La Jolla, CA 92093. Phone: (858)822-5610. Fax: (858)822-4566. E-mail: rklemke@ucsd.edu

   Brain development and spinal cord regeneration require neurite sprouting and growth cone navigation in response to extension and collapsing factors present in the extracellular environment. These external guidance cues control neurite growth cone extension and retraction processes through intracellular protein phosphorylation of numerous cytoskeletal, adhesion, and polarity complex signaling proteins. However, the complex kinase/substrate signaling networks that mediate neuritogenesis have not been investigated. Here, we compare the neurite phosphoproteome under growth and retraction conditions using neurite purification methodology combined with mass spectrometry. More than 4000 non-redundant phosphorylation sites from 1883 proteins have been annotated and mapped to signaling pathways that control kinase/phosphatase networks, cytoskeleton remodeling, and axon/dendrite specification. Comprehensive informatics and functional studies revealed a compartmentalized ERK activation/deactivation cytoskeletal switch that governs neurite growth and retraction, respectively. Our findings provide the first system-wide analysis of the phosphoprotein signaling networks that enable neurite growth and retraction and reveal an important molecular switch that governs neuritogenesis.

   Neuritogenesis is a dynamic process involving the extension of long, thin protrusions called neurites that will subsequently differentiate into long axons or an elaborate dendritic arbor (1-4). This highly polarized process occurs through the segmentation from the soma periphery of a microtubule-rich shaft capped with a growth cone, which itself is characterized by an actin-rich lamellipodium with numerous filopodial extensions and integrin-mediated adhesive contacts. Understanding this process is crucial as it is necessary for proper wiring of the brain and nerve regeneration, and has been linked to numerous neurodegenerative diseases.

   Although cultured neurons randomly form neurites in vitro, in vivo this process is orchestrated by gradients of chemoattractants, extracellular matrix proteins, and collapsing factors that precisely guide neurite initiation and advancement (5,6). This occurs in a polarized and highly controlled manner and relies on spatially regulated mechanisms for gradient sensing, membrane trafficking, integrin-mediated adhesion, and organization of the actin-microtubule cytoskeleton (5-8). These events are largely orchestrated by numerous surface guidance/repulsion and adhesion receptors that signal to the cell interior through multiple kinase activation and substrate phosphorylation events (7,9-17). Protein phosphorylation is a critical posttranslational modification that regulates

1

protein-protein interactions, enzymatic activity, and subcellular localization. The reversible addition of PO^{-4} to serine, theronine, and tyrosine amino acid residues is mediated by more than 500 kinases and over 150 phosphatases (18-20). In many cases, kinases phosphorylate specific amino acids in the context of a consensus recognition sequence. For example ERK is a proline directed kinase that phosphorylates S/T residues with the consensus sequence PxS/TP where x can be a neutral or basic amino acid (21-24). The identification of phosphorylation sites in the context of a specific kinase recognition sequence of given substrate has proven quite useful in the predication of kinase activation events in the cell (25-27). Also, kinases themselves can be phosphorylated at specific sites that are known to promote enzymatic activation which can be used to predict kinase activity in the cell. This is further enriched by computational models that predict higher order contextual features of kinases such as protein scaffolding, subcellular localization, and expression patterns (13,25-28). When combined, in silico programs have been shown to predict kinase activity with significant accuracy. This approach has been applied to large phosphoproteomic data sets consisting of thousands of phosphorylation sites revealing important kinase signaling networks that modulate cell migration, DNA damage, and yeast biology (13,25,29,30).

While significant progress has been made in identifying specific signals regulating neuritogenesis, a system-wide analysis of the phosphoprotein signals that control this process has not been investigated. Consequently, our understanding of the complex kinase/substrate signaling networks that regulate neurite formation and guidance are not defined. Here we describe a microporous filter method that facilitates selective purification of neurites undergoing growth or retraction. This fractionation method combined with immobilized metal-ion affinity chromatography (IMAC) and LC-MS protein identification technologies facilitated the identification of thousands of protein phosphorylation signatures that mediate neurite extension or retraction events induced by growth promoting or collapsing stimuli, respectively. Functional annotation and kinase activity predications in silico reveal phosphoprotein

networks controlling cytoskeletal remodeling, axon/dendrite specification, and cell adhesion. Kinase signaling analysis and cell-based assays revealed that an integrin/MEK/ERK signaling pathway operates as a critical switch controlling neurite extension and retraction dynamics.

EXPERIMENTAL PROCEDURES

Antibodies and reagents. Lysophosphatidic acid (Sigma). ROCK inhibitor Y-27632 (Sigma) and ERK kinase inhibitor PD98059 (Calbiochem). Alexa-fluor 488 labeled phalloidin (Invitrogen). DM-1A Anti α-tubulin antibodies and alexa-fluor 546 conjugated secondary antibodies (Sigma). C14 anti-erk antibody (Santa Cruz). Anti-p130CAS (Cell Signaling or Santa Cruz). Anti-Cdc42, -Rac antibodies (Millipore). Phospho-MEK1 S298 and T292, and anti-phospho-ERK-TEY antibodies (Biosource). Anti-MEK1 and Crk antibody (BD Transduction). Phospho-MEK1/2 S218/S222 antibody (Cell Signaling). Anti-myosin light chain and anti-phospho-myosin light chain serine 19 antibodies (Sigma). Anti-Akt and anti-phospho-Akt-S473 (Cell Signaling). Anti-phosphotyrosine 4G10 (Millipore). Anti-Abl kinase antibody (Sigma). Anti-FAK (Santa Cruz) and anti-phospho-FAK-Y397 antibody (Biosource). All MEK constructs have been previously described and were kindly provided by Dr. Andrew Catling (Louisiana State University Health Sciences Center, New Orleans, LA) (31-34).

Purification of growing and retracting neurites. Procedures for the culturing and biochemical preparation of extending neurites from NIE-115 cells using 3.0 μm microporous filters were the same as described before (35). To purify retracting neurites, NIE-115 cells were allowed to extend neurites for various times (8-24 hours) towards laminin (10 μg/ml, Millipore) then LPA (1μM) was added to the media in either the upper or lower chamber to induce retraction for the times indicated in the text. Extending or retracting neurites or their corresponding cell bodies were differentially harvested into lysis buffer for biochemical analyses as described (35). For GTPase activity assays, lysates were prepared as previously described (35). To block LPA-induced neurite retraction 10 μM Y-27632 was added to

the chamber for 60 minutes prior to LPA stimulation. To block ERK activation, 25 μM PD98059 was added to the chamber for the indicated times. Transient transfection of NIE-115 with the plasmids, neurite imaging, and immunofluorescence of the neurite cytoskeleton was performed as described (35). To prepare samples for proteomics analysis, extending or retracting neurites or their corresponding cell bodies were differentially harvested into lysis buffer of freshly made 7M Urea, 0.5% NP-40 in 50 mM ammonium bicarbonate (pH 8.0) containing 50 nM calyculin A and 0.2 mM vanadate as phosphatase inhibitors. After incubation on ice for 30 minutes, insoluble matter was removed by centrifugation at 16,000 g for 20 minutes.

Phosphopeptide Enrichment and Capillary HPLC-MS/MS Analysis. Protein samples (five biological replicates each for both extending and retracting neurites) were digested with trypsin at room temperature. Tryptic peptides were desalted and methyl esterified (250 μg for each sample), followed by immobilized metal-ion (Fe^{3+}) affinity chromatography (IMAC) to enrich phosphopeptides, as detailed in the recent report(36). After IMAC enrichment, aliquots (1/6 of the IMAC elution) were analyzed on a ThermoElectron LTQ-Orbitrap (Waltham, MA) coupled to an automated dual-column phosphoproteome nano-HPLC platform assembled in-house. The LC gradient (A = 100 mM HOAc in H_2O, B = 70% acetonitrile/100 mM HOAc in H_2O) was 0-70% B for ~180 min. For each sample, two technical replicates of LC-MS analyses were performed (36).

Database search and peptide identification. Phosphopeptides were identified from MS/MS spectra using SEQUEST by searching against the mouse IPI database. For confident phosphopeptide identifications, the false discovery rate (FDR) at peptide spectrum level was controlled at ≤ 0.5 % using in-house developed software (37). This program also measured the probability of correct phosphorylation site localization in each identified peptide by calculating the AScore for each phosphorylation site (38), and the assigned top phosphopeptide sequence was taken as the final peptide identification for a given spectrum.

Evaluation of phosphopeptide changes in growth and retracting neurite. We applied the spectral count method to evaluate the changes of phosphopeptides. The total spectral counts for each identified phosphopeptide in each neurite condition and their ratios were used to semi-quantitatively estimate their abundance in each condition (39).

Bioinformatics. The pathway analysis was performed using the Ingenuity Pathway Analysis software (Ingenuity Systems, http://www.ingenuity.com) as previously described (48). Briefly, we queried all phosphoproteins against the IPKB to search all possible pathways that could be represented by the query proteins. The significance of each pathway was evaluated by the right-tailed Fisher's Exact, which measures how likely it is the query proteins are relevant to the pathway. For the kinase-phosphorylation substrate relationship analysis, we used NetworkIN software to assign possible kinases to each identified site (25). The data used for the analysis was pre-formatted using in-house software to meet the format requirement of NetworkIN (http://networkin.info/newPrediction.php).

RESULTS

Model system for purification of growing and retracting neurites. Our previous work has shown that extending neurites can be purified from the cell body of NIE-115 cells using culture chambers equipped with 3.0 μm microporus filters (Fig.1A) (35). We utilized these NIE-115 cells because they can be grown in large numbers for large-scale biochemical analysis and have been well characterized for their neuron-like properties. Laminin was coated on the bottom of the filter which serves as a potent and directional cue for neurite initiation (35,40-42). Neurite extension through the pore to the lower surface of the filter is β1-integrin dependent and occurs in a highly directional and polarized manner (35). Therefore, because the cell body remains on the surface of the filter and neurite growth occurs exclusively through the pore to the lower surface, it is possible to selectively purify this structure from the polarized neuron for spatial proteomic analysis. Neurite growth under these conditions is linear for up to 24 hours, reaching a maximum around 36-48 hours after plating (Fig. 1A-C). The optimal time

3

to harvest extending neurites for biochemical analyses was 18-20 hours post plating on the laminin coated filters. At this time the majority of neurites are elongating, have well defined growth cones, and provide sufficient amounts of neurite protein for MS analysis. To obtain retracting neurites, we added the collapsing factor, LPA, to the lower chamber containing neurites that had been allowed to extend to the lower surface for 18 hours (43-45). The kinetics of retraction is shown in Fig. 1D. Retracting neurites were harvested 10-15 minutes after LPA stimulation because the majority of neurites were in the process of retraction and sufficient amounts of neurite protein can still be obtained from the filter at this time. It is notable that applying LPA selectively to the cell bodies on the upper chamber surface did not significantly induce neurite retraction. These findings indicate that the neurite and soma compartments of polarized neurons are spatially sensitive to this collapsing agent through an unknown mechanism. The spatial sensitivity to guidance cues like LPA is indicative of highly polarized neurons (5-7,17,46-51). Also, the neurite purification system is amenable to other cells and ECM proteins including pheochromocytoma PC12 cells on fibronectin and laminin (35). These findings together with our previous work indicate that the microporous system provides a robust method to selectively purify growing or retracting neurites.

Comparison of the neurite phosphoproteomes from growing and retracting neurites. The ability to selectively purify growing or retracting neurites independent of the soma provided a unique opportunity to study the phosphorylation/dephosphorylation mechanisms and kinase networks governing neuritogenesis in a highly spatial manner. To quantify relative changes in specific phosphorylation sites in purified growing and retracting neurites, we used immobilized metal-ion affinity chromatography to capture phosphopeptides and a liquid chromatography-mass spectrometry platform to identify parent proteins and their sites of phosphorylation as described in Experimental Procedures (52-56). In total 3512 phosphopeptides were identified by MS/MS from growing and retracting neurites, representing 1883 phosphoproteins and 4145 non-redundant phosphorylation sites (sTable 1). Of these peptides,

2676 were singly phosphorylated and 836 were doubly or multiply phosphorylated. The protein identifications and sites of phosphorylation were confidently assigned with an FDR of 1%.

A change in a specific phosphorylation site(s) within a phosphopeptide, was considered significant with a total spectral count of 2 or more and if it either increased or decreased by at least 1.5 fold or uniquely identified in the growing or retracting neurite fraction. All other phosphorylation sites were considered equally abundant with no specific change in both conditions. Before evaluating of the relative abundance of a specific phosphopeptide in growing or retracting neurites, we first filtered the phosphopeptide dataset to remove redundancy because some peptides from the same protein may contain exactly the same phosphorylation sites due to miscleavage during tryptic digestion. After removing the redundancy, we obtained a total of 3203 phosphopeptides with unique phosphorylation status, i.e., even two peptides with the same amino acid sequences from the same protein must have different phosphorylation sites. The growth to retraction ratios of all phosphorylation sites are shown in sTable 1. Using these criteria, 513 phosphopeptides were increased in growing neurites, 368 phosphopeptides were increased in retracting neurites, and 543 phosphopeptides were equally abundant. In total, 531 proteins were observed to have altered phosphorylation sites (> or < 1.5 fold) in response to neurite extension and retraction.

Functional annotation of phosphoproteins involved in neurite growth and retraction. To find the functional interrelationship and assign the identified phosphoproteins that change during growth and retraction to their signaling pathways, we used the Ingenuity Pathways Analysis (IPA) program and the Knowledge Base IPKB. IPA is a system wide database of biological pathways created from multiple relationships of proteins, genes, and diseases. The IPA program can analyze large genomic or proteomic datasets to find the most statistically significant canonical pathways and protein networks relevant to the dataset based on the calculated probability score by searching the IPKB. Of a total of 78 pathways identified RhoA signaling was the most highly represented during the growth and retraction of the neurite (Fig. 2, sFig.1). This was expected as RhoA

4

signaling has been shown to play a prominent role in mediating neurite retraction in response to various collapsing factors including LPA (17,44,45,57-59). Also, given that the cytoskeletal remodeling is a key event during neurite growth and retraction it is not surprising that many pathways that regulate the cytoskeleton were highly represented including the small GTPases Rac, RhoA, and Cdc42, as well as integrin signaling, ILK, and FAK (1,7,8,17,35,46,47,60-66). Furthermore, it is notable that ERK, PI3K, PKA kinase signaling are highly represented as these pathways are known to control cytoskeleton remodeling (66-74). Interestingly, in our previous work we reported that integrin and cytoskeleton-associated proteins were also the most abundant proteins represented in the neurite compared to the soma compartment (35). Thus, cytoskeletal proteins are highly enriched in the neurite and are the major targets modified by phosphorylation during neurite growth and retraction. Together these findings highlight the significance of using neurite purification methodology and phosphoprotein profiling to reveal signaling pathways that control neurite growth and retraction in a highly spatial manner.

Assignment of Identified Phosphorylation Sites to Known Kinases. To determine the kinases responsible for phosphorylation of neurite proteins, we utilized NetworKIN, an integrative computational approach that greatly augments kinase motif-based approaches by using contextual information to enhance kinase-substrate assignments (25,28). The contextual information is integrated from curated pathway databases, protein interaction assays, scaffolding, co-occurrence in abstracts, physical protein interaction assays, mRNA expression studies, subcellular localization, and genomic context. Combining the contextual information with existing matrices that identify kinase domain recognition motifs has been shown to improve the accuracy of kinase-substrate assignments by 2.5 fold. Using this approach, we were able to assign specific kinases to 73.3% (737 out of 1006) of the phosphorylation sites that change during neurite growth or retraction (Fig. 3). Of the 82 different kinases assigned to this process, PKACA, BTK, MAPKAPK5, MAP2K4 (ERK), and PDGFRβ kinases showed the highest ratio for the number of substrate phosphorylations in the extending neurite versus retracting neurites, whereas ZAP70, PRKCZ, PRKACG, LCK showed the lowest ratio.

ERK/MEK and RhoA signaling are spatially regulated during neurite growth and retraction. Our computational analyses indicate that MEK/ERK (MAP2K4) and RhoA signaling are highly modulated in growing/retracting neurites (Fig. 2, 3, and sFig. 1). Because the role of ERK and RhoA signaling in controlling neurite dynamics are poorly understood, we investigate these signaling pathways in more detail (40,67,75-81). We first directly monitored MEK and ERK kinase activities in the soma/neurite fractions using Western blotting and phosphospecific antibodies that report kinase activities of these proteins due to phosphorylation of MEK-S218/S222 and ERK TEY sequence (Fig. 4A). Both ERK and MEK kinase activities are highly increased in the extending neurite compared to the soma. The total level of ERK protein was the same in the soma and neurite compartments while total MEK protein was slightly increased in the neurite. These findings demonstrate that MEK/ERK activity is highly compartmentalized to the neurite during formation of this structure. Interestingly, LPA-mediated neurite collapse induced a rapid decrease in ERK and MEK activities, which correlated with neurite retraction kinetics (Fig. 4, A and B). In contrast, Akt activity was not inhibited by LPA-induced neurite retraction (Fig. 4C). These findings demonstrate that in polarized neurons MEK/ERK kinase activity is highly compartmentalized within the neurite and that during neurite collapse MEK/ERK activity is shut off.

Integrins spatially regulate MEK phosphorylation/activation during neurite growth and retraction. We next investigated how MEK activity and its known regulators are spatially organized in growing and retracting neurites to mediate compartmentalized ERK activity. Because we previously showed that β1 integrins drive directional neurite extension toward laminin in this model, we wanted to know if integrins played a role in MEK/ERK activation (35). During cell adhesion and membrane spreading MEK1 activity has been shown to be regulated by integrin signals that promote phosphorylation of threonine 292 (T292, human) and serine 298 (S298, human) (31-34). Integrins activate the small GTPases Rac and Cdc42, which activate PAK kinase, which in turn

5

phosphorylates MEK-S298 leading to increased catalytic activity towards ERK. Interestingly, current evidence indicates that phosphorylation of MEK-T292 by ERK itself negatively regulates MEK activity by decreasing PAK's ability to phosphorylate MEK-S298. This reduces the efficiency of MEK activity towards ERK, thereby reducing its kinase activity. In this way ERK-mediated phosphorylation of MEK-T292 serves as a negative feedback loop for self-regulation. However, the role of integrin/Rac/Cdc42/PAK to MEK-T292/S298 phosphorylation in neurite formation has not been investigated to date.

Interestingly, in the soma we observed low levels of MEK-S298 phosphorylation that was concomitant with a high level of MEK-T292 phosphorylation (Fig 4A). Conversely, in the extending neurite the level of MEK-T292 phosphorylation was decreased relative to the level of MEK S298 phosphorylation, which is consistent with the high level of ERK activity in this compartment (Fig. 4A). The increased ratio of MEK T292/S298 phosphorylation relative to the small pool of activated ERK present in the soma indicates that MEK activity is strongly inhibited in the soma due to the negative feedback modulation by ERK. These findings are consistent with the idea that the low level of ERK activity in the soma (Fig. 4A) results from the uncoupling of PAK from MEK-S298 phosphorylation. On the other hand, negative feedback modulation of MEK by ERK in the neurite is significantly attenuated leading to robust MEK-S298 phosphorylation and increased ERK kinase activity. Thus, in the neurite MEK/ERK activity is robust and strongly coupled to integrin/PAK signaling whereas in the soma ERK activity is low and not uncoupled to integrin/PAK signaling, due to strong negative feedback modulation by ERK. These findings suggest that integrins drive directional neurite extension through compartmentalized PAK/MEK/ERK signaling. These findings are further supported by the observation that Cdc42 and Rac activities are significantly elevated in the neurite compared to the soma (Fig. 4D). We also detected several PAK family members (1, 2, 4) which are present in the neurite and modified by phosphorylation (sTable 1).

LPA-induced neurite collapse disrupts integrin/PAK/Rac/Cdc42/MEK/ERK signaling. In the neurite, the level of S298 phosphorylation

decreased in response to LPA-induced collapse, which correlated with the loss of ERK, Cdc42, and Rac activities (Fig. 4A-D). As expected, MEK-T292 phosphorylation by ERK decreased in response to the loss of ERK activity (Fig. 4A). These findings suggest that LPA induces neurite collapse and ERK activity by interfering with integrin adhesion signaling to Rac/Cdc42/PAK and MEK-S298 phosphorylation. In support of these findings, LPA blocked ERK activation and MEK S298 phosphorylation induced by integrin-mediated NIE-115 cell attachment and spreading on laminin (Fig. 4G). In addition, LPA was found to modulate tyrosine phosphorylation of several known integrin/focal adhesion-associated proteins (FAK, CAS, Abl, Lasp-1, Crk) (Fig. 4, E and F)(82-85). It is also notable that LPA treatment decreased CAS phosphorylation, while it increased Crk Y221 phosphorylation, and Abl/Arg tyrosine phosphorylation (Fig. 4E). These phosphorylation events have been previously associated with decreased CAS/Crk coupling and Rac activity in spreading cells downstream of integrin receptors (83-85). Taken together these findings suggest that neurite extension involves integrin activation of the CAS/Crk/Rac/Cdc42/PAK/MEK-S298/ERK signaling pathway, whereas LPA-induced collapse blocks activation of integrin signaling leading to neurite detachment and retraction from the substrate.

Integrin Regulation of MEK/ERK activity is necessary for neurite growth and retraction. To investigate the functional significance of MEK/ERK activity in neuritogenesis, we expressed mutationally activated MEK (MEK-S211E/S222E, catalytically active MEK, MEK-CA) in cells and then examined neurite formation towards laminin (Fig. 5, A and D). This phosphomimetic mutation promoted constitutive ERK activation and increased neurite formation (Fig 5A). Interestingly, substitution of S298 with an alanine residue in MEK-CA partially reduced neurite formation suggesting that this site of phosphorylation does contribute to MEK/ERK-induced neurite formation even when MEK is constitutively activated. In contrast, MEK-CA with T292 mutated to alanine increased neurite formation probably because MEK is no longer susceptible to negative feedback regulation by ERK (Fig. 5A). MEK kinase activity was required

6

for neurite formation, since treatment of cells with the MEK inhibitor PD98059 blocked ERK activation and neurite formation on laminin (Fig. 5B). These findings indicate that MEK activation is sufficient and necessary to induce neurite formation and this response is partially regulated by MEK-S298/T292 phosphorylation.

Inhibition of MEK/ERK activity is necessary for RhoA/ROCK/MLC-mediated neurite retraction. We next investigated whether MEK/ERK inactivation is required for neurite retraction. NIE-115 cells expressing a mutationally active form of MEK1 (MEK-CA) were treated with LPA and monitored for neurite retraction and ERK kinase inactivation. Strikingly, LPA did not induce neurite retraction or inhibit ERK activation in MEK-CA cells, nor did it prevent S298 phosphorylation (Fig. 5, C and D). The fact that phosphorylation of MEK-S298 is not inhibited by LPA treatment in MEK-CA cells suggests that ERK activation provides a positive feedback mechanism to maintain integrin/Rac/Cdc42/PAK signaling in the neurite, thereby, preventing neurite detachment and retraction from the ECM. Interestingly, while inhibition of MEK/ERK activity with PD98059 did not induce neurite retraction by itself, it did increase retraction induced by a suboptimal dose of LPA (50% of the maximum) (Fig. 5E). Thus, while the loss of ERK activity is not sufficient to induce neurite retraction per se, it does sensitize the cell to LPA-mediated retraction. These findings suggest that LPA-induced neurite retraction not only requires ERK deactivation, but also involves activation/deactivation of additional signaling pathways. RhoA activation is a likely candidate since LPA-induced neurite retraction requires RhoA activation, which facilitates ROCK-mediated myosin contraction (sFig.1) (7,17,57,86-88). Consistent with these observations, the ROCK kinase inhibitor Y-27632 prevented neurite retraction and myosin contraction as indicated by a decrease in serine 19 phosphorylation of myosin light chain (Fig. 6, A and B)(7,88). Importantly, Y-27632 not only prevented neurite retraction, but also blocked LPA-induced ERK deactivation and MEK-S298 phosphorylation in the neurite fraction (Fig. 6B). Thus, inhibition of integrin/RacCdc42/PAK/MEK/ERK signaling is necessary for LPA-RhoA/ROCK/MLC-mediated neurite retraction. Based on our functional proteomics work and the work of others we proposed a model for how neurites extend and retract in response to laminin and LPA. The model is shown schematically in figure 6C and sFig.1 and is discussed below.

DISCUSSION

Our ability to differentially isolate neurites in a state of growth or retraction for proteomic analyses provided a simple and robust system to globally profile thousands of protein phosphorylation and kinase changes that mediate neuritogenesis. An important aspect of this model system is the ability to specifically isolate the neurite from the soma for proteomic analyses. This unique strategy allowed us to mine deeper into the neurite phosphoproteome uncovering many more low abundant phosphoproteins. Because of this, we were able to obtain a more precise picture of the complex spatial kinase/substrate networks that control neurite growth/retraction kinetics. Also, the neurite purification methods described here will likely transfer to other neuronal cell types, guidance factors and collapsing agents. For example, we have previously reported that neurites can be readily purified from PC12 cells responding to laminin and fibronectin guidance cues (35). It may also be possible to selectively purify axons and dendrites from primary neurons for detailed proteomic analyses using specific differentiation and/or guidance factors. In any case, the utility of this model system combined with the rapid progress being made in quantitative mass spectrometry will help provide a more comprehensive understanding of the neurite proteome and its spatial organization, which, in turn, will provide valuable insight into the various disease pathologies caused by deregulation of this process.

Using NetworKIN, we find that a large panel of kinases are active during neurite growth, whereas a relatively reduced number of kinases are active during retraction. Many of these kinases have been previously implicated in the regulation of different aspects of neurite outgrowth. PKA (*PKACA*) can trigger neurite outgrowth by phosphorylating synapsins (89) and CREB (90). The MET receptor (*MET*) enhances axonal outgrowth of cultured dorsal root ganglions by

7

potentiating NGF signaling (91). The tyrosine kinase BTK (*BTK*) phosphorylates the actin regulator N-WASP which is essential for neurite outgrowth (92). The cyclin kinase Cdk5 (*CDK5*) regulates neurite and axon outgrowth by phosphorylating the kinase PAK1 and the microtubule associated protein MAP1B (93). GSK3 (*GSK3A*) phosphorylates the collapsin response mediator protein-2 (CRMP-2) to promote neurite elongation via microtubule assembly (94). The MAP kinase kinase MKK4 (*MAP2K4*) and its substrate JNK (*MAPK9*) have also been involved in the regulation of neurite outgrowth through the phosphorylation of the microtubule binding proteins MAP, MAP1, doublecortin and SGC10 (95). Although these findings point to a wide array of kinase classes that regulate neuritrogenesis, it is likely that they work together in time and space to fine tune changes in the actin and microtubule cytoskeletons that drive this process. Using similar proteomics and bioinformatic methods, we recently revealed a Rho GTPase signaling network that regulates neurite outgrowth (35). This allowed us to uncover an unexpected signaling complexity, with different Rho GTPase signaling modules operating in time and space to regulate distinct neurite functions including neurite initiation, elongation, pathfinding and filopodial stabilization. Similarly, the wide kinase activation and signal annotation profiles we observe hint to a high degree of modularity in fine tuning neuritogenesis. On the other hand, the precise functions of the protein kinases that modulate LPA-induced neurite collapse were less clear from our phosphoproteomic datasets. However one of these kinases, Serum- and Glucocorticoid-Inducible Kinase 1 (SGK), regulates microtubule depolymerization and the shortening of neuronal processes (96). It will be important in the future to systematically probe these different kinase-substrate networks to reveal their specialized contribution to the dynamic processes of neurite growth and retraction.

Our combined informatics and functional studies revealed that integrin to MEK/ERK signaling plays a prominent role in controlling neuritogenesis. Based on our findings and the work of others we have constructed a working model for how MEK/ERK activation and deactivation by LPA control neuritogenesis (figure 6C). The signaling components that were used to construct the schematic and their relative abundance in the soma and neurite as well as their observed phosphorylation sites are listed in figure 6C and sTable 3. Part (a) shows the proposed pathway for how integrins mediate ERK activation leading to neurite extension. ECM proteins like laminin and fibronectin are present as adhesive gradients in the extracellular environment that can initiate and guide neurite protrusion from the cell body through activation of integrin receptors and the recruitment of their downstream effectors including FAK/CAS/Crk (8,83,84). This canonical pathway operates spatially in the neurite to drive localized Rac activation of PAK. PAK then phosphorylates MEK S298 leading to enhanced MEK and ERK activity as described in non-neuronal cells (31-34). The integrin/Rac/PAK/MEK-S298 signaling cascade promotes strong sustained ERK activation, which serves as a switch to mediate neurite outgrowth, while suppressing basal RhoA/ROCK/MLC-mediated membrane contractility, possibly through PKA activation (Part b).

Although the spatial mechanisms that promote localized ERK activation in the neurite are not clear the integrin/Rac/PAK activation pathway most likely works in close conjunction with common upstream activators of MEK including Rap-1, Ras and Raf (22,97-102). These upstream signals fully activate MEK through phosphorylation of S218/S222 (103,104). It is notable that although MEK activation may occur through either B-Raf and/or Raf-1 activation, our phosphoproteomics work suggests that B-Raf is more likely involved since Raf-1 is highly phosphorylated on S43 (growth specific) in extending neurites (sTable 1). S43 phosphorylation has previously been associated with PKA activation and is inhibitory to Raf-1 kinase activity (105,106). How then is B-Raf activity modulated to increase MEK/ERK signaling? Integrin activation of Rap-1 can modulate B-Raf activity as can cAMP/PKA signaling (102). Rap1A and B isoforms are present in the neurite and several Rap1 GEF and GAP effector proteins are differentially phosphorylated during neurite growth and retraction (sTable 1). Rap activity and its effectors could be modulated directly or indirectly by integrin activation and/or cell spreading on laminin, possibly through PKA activation (102).

8

Alternatively, integrin activation of FAK/Src can facilitate activation of the canonical Grb2/SOS/Ras/Raf/MEK/ERK pathway(22). In the end, ERK activity self regulates by modulation of its upstream activators through negative feedback phosphorylation of MEK-S292, which suppresses PAK phosphorylation of 298 and phosphorylation of B-Raf-S151, which inhibits B-Raf activity (102). Part (c) shows a list of cytoskeletal effector proteins that are either known and/or predicted to be phosphorylated by ERK and, thus may modulate neurite growth. Of particular interest are α-parvin, which modulates focal adhesion and actin cytoskeletal dynamics and the microtubule modulating proteins crmp-1, MARK2, MAP1B, and MAP2 (10,107-109). sTable 2 shows a complete list of all identified phosphoproteins with ERK consensus phosphorylation signatures.

An important finding in our study was that LPA could disrupt integrin signaling leading to blockade of the CAS/Crk/Rac/PAK/MEK/ERK pathway (Part a and b). We suspect that this facilitates neurite detachment from the ECM by losing integrin adhesions to the substratum while activating the Rho/ROCK contractile mechanisms that physically mediate growth cone collapse and membrane retraction through force generation (Fig. 6C and sFig. 1) (7). Interestingly, the RhoA/ROCK/MLC pathway has been reported to mediate neurite collapse by modulating collapsin response mediator protein (Crmp) family proteins and microtubule dynamics (5,108-110). In our work here, Crmp-1 was observed to be enriched by 7-fold in the neurite and to be differentially phosphorylated on multiple sites in neurites undergoing growth or retraction (sTable 1). Although the mechanisms that block LPA-induce integrin signaling in the neurite are not defined, Abl family kinases (Abl and Arg) are likely to play a central role through their ability to modulate CAS/Crk coupling and Rac activity at adhesion sites as described (8,83-85,111-113).

Importantly, we found that Abl is hypertyrosine phosphorylated and enriched by 7-fold in the neurite. Also, Abl itself and its known substrates c-CrkII-Y221 and LASP-1 show increased phosphorylation in the neurite in response to LPA (Fig. 4E)(82). This suggests that LPA activates Abl kinase which in turn tyrosine phosphorylates Crk at Y221 inhibiting CAS/Crk coupling and downstream Rac/PAK/MEK activation. It is also notable that LPA did not inhibit MEK-S298 phosphorylation by PAK in cells expressing constitutively activated MEK, which was associated with decreased neurite retraction (Fig. 5, A and D). This suggests that MEK/ERK signaling provides a positive feedback to maintain integrin/CAS/Crk/Rac/PAK signaling and, thus, prevent neurite retraction.

Taken together our work and the work of others suggest a model whereby the net effect of high Rac/PAK/MEK/ERK activation and RhoA inhibition is increased membrane protrusion and decreased neurite contraction events leading to net neurite growth. Increased Rac activity has been shown to suppress RhoA signaling which leads to neurite growth in neurons (7,114). PKA and ERK signaling can also suppress RhoA signaling in other cell types (115-117). On the other hand, LPA strongly activates RhoA/ROCK/MLC and Abl kinase which together mediate neurite detachment from the ECM and membrane contraction leading to growth cone turning and/or collapse. In this model Rac/PAK/MEK/ERK signaling serves as a spatially compartmentalized switch that operates downstream of integrin and LPA receptor activation to modulate neurite growth and retraction kinetics, respectively. Our findings provide a plausible mechanism for how neuronal growth cones spatially interpret extracellular cues and navigate through complex tissues, which is critical for proper brain development and spinal cord regeneration.

REFERENCES

1.   Giannone, G., Mege, R. M., and Thoumine, O. (2009) *Trends Cell Biol* **19**(9), 475-486
2.   Drees, F., and Gertler, F. B. (2008) *Curr Opin Neurobiol* **18**(1), 53-59
3.   Koh, C. G. (2006) *Neurosignals* **15**(5), 228-237
4.   Allen, J., and Chilton, J. K. (2009) *Dev Biol* **327**(1), 4-11
5.   Arimura, N., and Kaibuchi, K. (2005) *Neuron* **48**(6), 881-884

6. Fukata, M., Nakagawa, M., and Kaibuchi, K. (2003) *Curr Opin Cell Biol* **15**(5), 590-597

7. Nikolic, M. (2002) *Int J Biochem Cell Biol* **34**(7), 731-745

8. Dent, E. W., and Gertler, F. B. (2003) *Neuron* **40**(2), 209-227

9. Jeon, S., Park, J. K., Bae, C. D., and Park, J. (2010) *Neurochem Int* **56**(6-7), 810-818

10. Dehmelt, L., and Halpain, S. (2007) *Curr Biol* **17**(15), R611-614

11. Yamauchi, J., Miyamoto, Y., Sanbe, A., and Tanoue, A. (2006) *Exp Cell Res* **312**(15), 2954-2961

12. Nusser, N., Gosmanova, E., Makarova, N., Fujiwara, Y., Yang, L., Guo, F., Luo, Y., Zheng, Y., and Tigyi, G. (2006) *Cell Signal* **18**(5), 704-714

13. Jorgensen, C., Sherman, A., Chen, G. I., Pasculescu, A., Poliakov, A., Hsiung, M., Larsen, B., Wilkinson, D. G., Linding, R., and Pawson, T. (2009) *Science* **326**(5959), 1502-1509

14. Round, J., and Stein, E. (2007) *Curr Opin Neurobiol* **17**(1), 15-21

15. Woodring, P. J., Litwack, E. D., O'Leary, D. D., Lucero, G. R., Wang, J. Y., and Hunter, T. (2002) *J Cell Biol* **156**(5), 879-892

16. Spencer, T. K., Mellado, W., and Filbin, M. T. (2008) *Mol Cell Neurosci* **38**(1), 110-116

17. Hirose, M., Ishizaki, T., Watanabe, N., Uehata, M., Kranenburg, O., Moolenaar, W. H., Matsumura, F., Maekawa, M., Bito, H., and Narumiya, S. (1998) *J Cell Biol* **141**(7), 1625-1636

18. Manning, G., Whyte, D. B., Martinez, R., Hunter, T., and Sudarsanam, S. (2002) *Science* **298**(5600), 1912-1934

19. Alonso, A., Sasin, J., Bottini, N., Friedberg, I., Osterman, A., Godzik, A., Hunter, T., Dixon, J., and Mustelin, T. (2004) *Cell* **117**(6), 699-711

20. Manning, G., Plowman, G. D., Hunter, T., and Sudarsanam, S. (2002) *Trends Biochem Sci* **27**(10), 514-520

21. Kim, E. K., and Choi, E.-J. (2010) *Biochim Biophys Acta* **1802**(4), 396-405

22. Yee, K. L., Weaver, V. M., and Hammer, D. A. (2008) *IET Syst Biol* **2**(1), 8-15

23. Ramos, J. W. (2008) *Int J Biochem Cell Biol* **40**(12), 2707-2719

24. Pullikuth, A. K., and Catling, A. D. (2007) *Cellular signalling* **19**(8), 1621-1632

25. Linding, R., Jensen, L. J., Ostheimer, G. J., van Vugt, M. A., Jorgensen, C., Miron, I. M., Diella, F., Colwill, K., Taylor, L., Elder, K., Metalnikov, P., Nguyen, V., Pasculescu, A., Jin, J., Park, J. G., Samson, L. D., Woodgett, J. R., Russell, R. B., Bork, P., Yaffe, M. B., and Pawson, T. (2007) *Cell* **129**(7), 1415-1426

26. Jorgensen, C., and Linding, R. (2010) *Curr Opin Genet Dev* **20**(1), 15-22

27. Tan, C. S., and Linding, R. (2009) *Proteomics* **9**(23), 5233-5242

28. Linding, R., Jensen, L. J., Pasculescu, A., Olhovsky, M., Colwill, K., Bork, P., Yaffe, M. B., and Pawson, T. (2008) *Nucleic Acids Res* **36**(Database issue), D695-699

29. Van Hoof, D., Munoz, J., Braam, S. R., Pinkse, M. W., Linding, R., Heck, A. J., Mummery, C. L., and Krijgsveld, J. (2009) *Cell Stem Cell* **5**(2), 214-226

30. van Vugt, M. A., Gardino, A. K., Linding, R., Ostheimer, G. J., Reinhardt, H. C., Ong, S. E., Tan, C. S., Miao, H., Keezer, S. M., Li, J., Pawson, T., Lewis, T. A., Carr, S. A., Smerdon, S. J., Brummelkamp, T. R., and Yaffe, M. B. (2010) *PLoS Biol* **8**(1), e1000287

31. Park, E. R., Eblen, S. T., and Catling, A. D. (2007) *Cellular signalling* **19**(7), 1488-1496

32. Eblen, S. T., Slack-Davis, J. K., Tarcsafalvi, A., Parsons, J. T., Weber, M. J., and Catling, A. D. (2004) *Mol Cell Biol* **24**(6), 2308-2317

33. Slack-Davis, J. K., Eblen, S. T., Zecevic, M., Boerner, S. A., Tarcsafalvi, A., Diaz, H. B., Marshall, M. S., Weber, M. J., Parsons, J. T., and Catling, A. D. (2003) *J Cell Biol* **162**(2), 281-291

34. Eblen, S. T., Slack, J. K., Weber, M. J., and Catling, A. D. (2002) *Mol Cell Biol* **22**(17), 6023-6033

35. Pertz, O. C., Wang, Y., Yang, F., Wang, W., Gay, L. J., Gristenko, M. A., Clauss, T. R., Anderson, D. J., Liu, T., Auberry, K. J., Camp, D. G., 2nd, Smith, R. D., and Klemke, R. L. (2008) *Proc Natl Acad Sci U S A* **105**(6), 1931-1936

10

36. Yang, F., Waters, K. M., Miller, J. H., Gritsenko, M. A., Zhao, R., Du, X., Livesay, E. A., Purvine, S. O., Monroe, M. E., Wang, Y., Camp, D. G., 2nd, Smith, R. D., and Stenoien, D. L. (2010) *PLoS One* **5**(11), e14152

37. Du, X., Yang, F., Manes, N. P., Stenoien, D. L., Monroe, M. E., Adkins, J. N., States, D. J., Purvine, S. O., Camp, D. G., 2nd, and Smith, R. D. (2008) *J Proteome Res* **7**(6), 2195-2203

38. Beausoleil, S. A., Villen, J., Gerber, S. A., Rush, J., and Gygi, S. P. (2006) *Nat Biotechnol* **24**(10), 1285-1292

39. Heibeck, T. H., Ding, S. J., Opresko, L. K., Zhao, R., Schepmoes, A. A., Yang, F., Tolmachev, A. V., Monroe, M. E., Camp, D. G., 2nd, Smith, R. D., Wiley, H. S., and Qian, W. J. (2009) *J Proteome Res* **8**(8), 3852-3861

40. Mruthyunjaya, S., Manchanda, R., Godbole, R., Pujari, R., Shiras, A., and Shastry, P. (2010) *Biochem Biophys Res Commun* **391**(1), 43-48

41. Plantman, S., Patarroyo, M., Fried, K., Domogatskaya, A., Tryggvason, K., Hammarberg, H., and Cullheim, S. (2008) *Mol Cell Neurosci* **39**(1), 50-62

42. Li, G. N., Liu, J., and Hoffman-Kim, D. (2008) *Ann Biomed Eng* **36**(6), 889-904

43. Sayas, C. L., Moreno-Flores, M. T., Avila, J., and Wandosell, F. (1999) *J Biol Chem* **274**(52), 37046-37052

44. Kranenburg, O., Poland, M., van Horck, F. P., Drechsel, D., Hall, A., and Moolenaar, W. H. (1999) *Mol Biol Cell* **10**(6), 1851-1857

45. Tigyi, G., Fischer, D. J., Sebok, A., Yang, C., Dyer, D. L., and Miledi, R. (1996) *J Neurochem* **66**(2), 537-548

46. O'Donnell, M., Chance, R. K., and Bashaw, G. J. (2009) *Annu Rev Neurosci* **32**383-412

47. Lowery, L. A., and Van Vactor, D. (2009) *Nat Rev Mol Cell Biol* **10**(5), 332-343

48. Xiang, Y., Li, Y., Zhang, Z., Cui, K., Wang, S., Yuan, X. B., Wu, C. P., Poo, M. M., and Duan, S. (2002) *Nat Neurosci* **5**(9), 843-848

49. Dickson, B. J. (2001) *Curr Opin Neurobiol* **11**(1), 103-110

50. Kalil, K., Szebenyi, G., and Dent, E. W. (2000) *J Neurobiol* **44**(2), 145-158

51. van Horck, F. P., Weinl, C., and Holt, C. E. (2004) *Curr Opin Neurobiol* **14**(1), 61-66

52. Liang, X., Fonnum, G., Hajivandi, M., Stene, T., Kjus, N. H., Ragnhildstveit, E., Amshey, J. W., Predki, P., and Pope, R. M. (2007) *J Am Soc Mass Spectrom* **18**(11), 1932-1944

53. Moser, K., and White, F. M. (2006) *J Proteome Res* **5**(1), 98-104

54. Brill, L. M., Salomon, A. R., Ficarro, S. B., Mukherji, M., Stettler-Gill, M., and Peters, E. C. (2004) *Anal Chem* **76**(10), 2763-2772

55. Ding, S. J., Wang, Y., Jacobs, J. M., Qian, W. J., Yang, F., Tolmachev, A. V., Du, X., Wang, W., Moore, R. J., Monroe, M. E., Purvine, S. O., Waters, K., Heibeck, T. H., Adkins, J. N., Camp, D. G., 2nd, Klemke, R. L., and Smith, R. D. (2008) *J Proteome Res* **7**(10), 4215-4224

56. Wang, Y., Ding, S. J., Wang, W., Jacobs, J. M., Qian, W. J., Moore, R. J., Yang, F., Camp, D. G., 2nd, Smith, R. D., and Klemke, R. L. (2007) *Proc Natl Acad Sci U S A* **104**(20), 8328-8333

57. To, K. C., Church, J., and O'Connor, T. P. (2008) *Neuroscience* **153**(3), 645-653

58. Sayas, C. L., Avila, J., and Wandosell, F. (2002) *Biochim Biophys Acta* **1582**(1-3), 144-153

59. Fukushima, N., Weiner, J. A., Kaushal, D., Contos, J. J., Rehen, S. K., Kingsbury, M. A., Kim, K. Y., and Chun, J. (2002) *Mol Cell Neurosci* **20**(2), 271-282

60. Tucker, B. A., Rahimtula, M., and Mearow, K. M. (2008) *Cell Signal* **20**(1), 241-257

61. Ivankovic-Dikic, I., Gronroos, E., Blaukat, A., Barth, B. U., and Dikic, I. (2000) *Nat Cell Biol* **2**(9), 574-581

62. Vogelezang, M., Forster, U. B., Han, J., Ginsberg, M. H., and ffrench-Constant, C. (2007) *BMC Neurosci* **8**44

63. Tahirovic, S., Hellal, F., Neukirchen, D., Hindges, R., Garvalov, B. K., Flynn, K. C., Stradal, T. E., Chrostek-Grashoff, A., Brakebusch, C., and Bradke, F. (2010) *J Neurosci* **30**(20), 6930-6943

64. Prager-Khoutorsky, M., and Spira, M. E. (2009) *Brain Res* **1251**65-79

65. Geraldo, S., and Gordon-Weeks, P. R. (2009) *J Cell Sci* **122**(Pt 20), 3595-3604

66. Quinn, C. C., and Wadsworth, W. G. (2008) *Trends Cell Biol* **18**(12), 597-603
67. Yasui, H., Ito, N., Yamamori, T., Nakamura, H., Okano, J., Asanuma, T., Nakajima, T., Kuwabara, M., and Inanami, O. (2010) *Free Radic Res* **44**(6), 645-654
68. Shelly, M., Lim, B. K., Cancedda, L., Heilshorn, S. C., Gao, H., and Poo, M. M. (2010) *Science* **327**(5965), 547-552
69. Wu, H., Ichikawa, S., Tani, C., Zhu, B., Tada, M., Shimoishi, Y., Murata, Y., and Nakamura, Y. (2009) *Biochim Biophys Acta* **1791**(1), 8-16
70. Desbarats, J., Birge, R. B., Mimouni-Rongy, M., Weinstein, D. E., Palerme, J. S., and Newell, M. K. (2003) *Nat Cell Biol* **5**(2), 118-125
71. Bordt, S. L., McKeon, R. M., Li, P. K., Witt-Enderby, P. A., and Melan, M. A. (2001) *Biochim Biophys Acta* **1499**(3), 257-264
72. Barnes, A. P., Solecki, D., and Polleux, F. (2008) *Curr Opin Neurobiol* **18**(1), 44-52
73. Piper, M., van Horck, F., and Holt, C. (2007) *Adv Exp Med Biol* **621**134-143
74. Shelly, M., Cancedda, L., Heilshorn, S., Sumbre, G., and Poo, M. M. (2007) *Cell* **129**(3), 565-577
75. Hollis, E. R., 2nd, Jamshidi, P., Low, K., Blesch, A., and Tuszynski, M. H. (2009) *Proc Natl Acad Sci U S A* **106**(17), 7215-7220
76. Nakata, H. (2007) *Biochem Biophys Res Commun* **355**(3), 842-848
77. Dimitropoulou, A., and Bixby, J. L. (2000) *Brain Res* **858**(1), 205-214
78. Perron, J. C., and Bixby, J. L. (1999) *Mol Cell Neurosci* **13**(5), 362-378
79. Kushner, S. A., Elgersma, Y., Murphy, G. G., Jaarsma, D., van Woerden, G. M., Hojjati, M. R., Cui, Y., LeBoutillier, J. C., Marrone, D. F., Choi, E. S., De Zeeuw, C. I., Petit, T. L., Pozzo-Miller, L., and Silva, A. J. (2005) *J Neurosci* **25**(42), 9721-9734
80. Elowe, S., Holland, S. J., Kulkarni, S., and Pawson, T. (2001) *Mol Cell Biol* **21**(21), 7429-7441
81. Perlson, E., Hanz, S., Ben-Yaakov, K., Segal-Ruder, Y., Seger, R., and Fainzilber, M. (2005) *Neuron* **45**(5), 715-726
82. Lin, Y. H., Park, Z. Y., Lin, D., Brahmbhatt, A. A., Rio, M. C., Yates, J. R., 3rd, and Klemke, R. L. (2004) *J Cell Biol* **165**(3), 421-432
83. Chodniewicz, D., and Klemke, R. L. (2004) *Exp Cell Res* **301**(1), 31-37
84. Chodniewicz, D., and Klemke, R. L. (2004) *Biochim Biophys Acta* **1692**(2-3), 63-76
85. Kain, K. H., and Klemke, R. L. (2001) *J Biol Chem* **276**(19), 16185-16192
86. Darenfed, H., Dayanandan, B., Zhang, T., Hsieh, S. H., Fournier, A. E., and Mandato, C. A. (2007) *Cell Motil Cytoskeleton* **64**(2), 97-109
87. Zhang, X. F., Schaefer, A. W., Burnette, D. T., Schoonderwoert, V. T., and Forscher, P. (2003) *Neuron* **40**(5), 931-944
88. Narumiya, S., Ishizaki, T., and Uehata, M. (2000) *Methods Enzymol* **325**273-284
89. Kao, H. T., Song, H. J., Porton, B., Ming, G. L., Hoh, J., Abraham, M., Czernik, A. J., Pieribone, V. A., Poo, M. M., and Greengard, P. (2002) *Nat Neurosci* **5**(5), 431-437
90. Vaudry, D., Stork, P. J., Lazarovici, P., and Eiden, L. E. (2002) *Science* **296**(5573), 1648-1649
91. Maina, F., Hilton, M. C., Ponzetto, C., Davies, A. M., and Klein, R. (1997) *Genes Dev* **11**(24), 3341-3350
92. Suetsugu, S., Hattori, M., Miki, H., Tezuka, T., Yamamoto, T., Mikoshiba, K., and Takenawa, T. (2002) *Dev Cell* **3**(5), 645-658
93. Paglini, G., and Caceres, A. (2001) *Eur J Biochem* **268**(6), 1528-1533
94. Yoshimura, T., Kawano, Y., Arimura, N., Kawabata, S., Kikuchi, A., and Kaibuchi, K. (2005) *Cell* **120**(1), 137-149
95. Haeusgen, W., Boehm, R., Zhao, Y., Herdegen, T., and Waetzig, V. (2009) *Neuroscience* **161**(4), 951-959
96. Yang, Y. C., Lin, C. H., and Lee, E. H. (2006) *Mol Cell Biol* **26**(22), 8357-8370
97. Pouyssegur, J., Volmat, V., and Lenormand, P. (2002) *Biochem Pharmacol* **64**(5-6), 755-763
98. Howe, A. K., Aplin, A. E., and Juliano, R. L. (2002) *Curr Opin Genet Dev* **12**(1), 30-35

12

99. McLeod, S. J., Shum, A. J., Lee, R. L., Takei, F., and Gold, M. R. (2004) *J Biol Chem* **279**(13), 12009-12019

100. Enserink, J. M., Price, L. S., Methi, T., Mahic, M., Sonnenberg, A., Bos, J. L., and Tasken, K. (2004) *J Biol Chem* **279**(43), 44889-44896

101. Kinbara, K., Goldfinger, L. E., Hansen, M., Chou, F. L., and Ginsberg, M. H. (2003) *Nat Rev Mol Cell Biol* **4**(10), 767-776

102. Retta, S. F., Balzac, F., and Avolio, M. (2006) *Eur J Cell Biol* **85**(3-4), 283-293

103. Alessandrini, A., Greulich, H., Huang, W., and Erikson, R. L. (1996) *J Biol Chem* **271**(49), 31612-31618

104. Pham, C. D., Arlinghaus, R. B., Zheng, C. F., Guan, K. L., and Singh, B. (1995) *Oncogene* **10**(8), 1683-1688

105. Gerits, N., Kostenko, S., Shiryaev, A., Johannessen, M., and Moens, U. (2008) *Cell Signal* **20**(9), 1592-1607

106. Dhillon, A. S., Meikle, S., Peyssonnaux, C., Grindlay, J., Kaiser, C., Steen, H., Shaw, P. E., Mischak, H., Eychene, A., and Kolch, W. (2003) *Mol Cell Biol* **23**(6), 1983-1993

107. Halpain, S., and Dehmelt, L. (2006) *Genome Biol* **7**(6), 224

108. Arimura, N., Menager, C., Kawano, Y., Yoshimura, T., Kawabata, S., Hattori, A., Fukata, Y., Amano, M., Goshima, Y., Inagaki, M., Morone, N., Usukura, J., and Kaibuchi, K. (2005) *Mol Cell Biol* **25**(22), 9973-9984

109. Inagaki, N., Chihara, K., Arimura, N., Menager, C., Kawano, Y., Matsuo, N., Nishimura, T., Amano, M., and Kaibuchi, K. (2001) *Nat Neurosci* **4**(8), 781-782

110. Arimura, N., Inagaki, N., Chihara, K., Menager, C., Nakamura, N., Amano, M., Iwamatsu, A., Goshima, Y., and Kaibuchi, K. (2000) *J Biol Chem* **275**(31), 23973-23980

111. Lanier, L. M., and Gertler, F. B. (2000) *Curr Opin Neurobiol* **10**(1), 80-87

112. Hernandez, S. E., Settleman, J., and Koleske, A. J. (2004) *Curr Biol* **14**(8), 691-696

113. Huang, J., Sakai, R., and Furuichi, T. (2006) *Mol Biol Cell* **17**(7), 3187-3196

114. Ehler, E., van Leeuwen, F., Collard, J. G., and Salinas, P. C. (1997) *Mol Cell Neurosci* **9**(1), 1-12

115. Mavria, G., Vercoulen, Y., Yeo, M., Paterson, H., Karasarides, M., Marais, R., Bird, D., and Marshall, C. J. (2006) *Cancer Cell* **9**(1), 33-44

116. Ehrenreiter, K., Piazzolla, D., Velamoor, V., Sobczak, I., Small, J. V., Takeda, J., Leung, T., and Baccarini, M. (2005) *J Cell Biol* **168**(6), 955-964

117. Stork, P. J., and Schmitt, J. M. (2002) *Trends Cell Biol* **12**(6), 258-266

ACKNOWLEDGEMENTS

The abbreviations used are: LC, liquid chromatography; MS, mass spectrometry; IMAC, immobilized metal-ion affinity chromatography; LPA, lysophosphatidic acid (Sigma); IPA, Ingenuity Pathways Analysis; IPKB, Ingenuity Pathways Knowledge base; PKA, protein kinase A; PDGFR, platelet derived growth factor receptor; FAK, focal adhesion kinase; CAS, p130crk-associated substrate; Abl, Abelson

tyrosine kinase; LASP-1, lim actin-associated protein one; ROCK, Rho-associated kinase; SOS, son of sevenless; Grb2, growth factor rector-bound protein 2. GEF, guanine nucleotide exchange factor, GAP, GTPase-activating protein; MARK2, microtubule–associated regulatory kinase 2; crmp-1, collapse response mediator protein 1; MAP, microtubule-associated protein; MLC, myosin light chain.

FIGURE LEGENDS

Fig. 1.   Characterization of neurite growth and retraction kinetics using 3.0 μm porous filters and the collapsing factor LPA. A. Schematic of a neurite purification chamber showing neurite extension toward the lower surface of the filter coated with laminin. B. Left panel, fluorescence photomicrograph of the lower surface of the membrane showing neurites stained with α-tubulin (red) extending through 3.0 μm pores toward a drop of laminin (green) for 18 hours. Note that neurites do not extend to the lower surface in the absence of laminin coating. Right panel, fluorescence photomicrograph of a NIE-115 neurite growth cone stained with FITC-phalloidin to visualize F-actin (green) and antibodies to tubulin to visualize microtubules (red). Bar, left panel 30 μm, right panel 10 μm.   C. Quantification of neurite extension kinetics to the lower surface of 3.0 μm membranes coated with laminin on the bottom only, top only, bottom and top, or not coated with laminin. Neurites were stained with crystal violet; the dye was eluted and quantified using a spectrophotometer as described in Experimental Procedures. Standard deviations from three independent experiments are shown. D.   Quantification of neurite retraction kinetics in response to LPA added to the lower chamber (left graph), upper or lower chamber (middle graph), or upper and lower chamber (right graph) for the indicated times.   E. Fluorescence photomicrograph of a time series of neurite retraction on the lower membrane surface in response to LPA added to the lower chamber for the indicated times. Arrow shows retracting neurites. Bar = 20 μm.

Fig. 2. Canonical pathways that are significantly represented by the identified phosphoproteins. 1775 out of 1883 identified phosphoproteins were mapped to the IPA database and used for pathways analysis. 78 pathways have a p-value lower than 0.05 as determined by Fishers's test. Shown are 28 of the most significant pathways.

Fig. 3. NetworKIN annotation of kinase substrates in growing and retracting neurites. The identified phosphosites in growing and retracting neurites were assigned to their cognate kinase class using the NetworKIN software program. The normalized ratio of the number of substrates for each kinase was calculated and only those that have more than two substrates and with the ratio > 1.5 or < -1.5 were shown for comparison.

Fig. 4. ERK kinase activation mediates NIE-115 neurite extension. A. Neurons were allowed to extend neurites through 3.0 μm pores toward laminin for 12 hours (growth) before LPA was added to the lower chamber for the indicated times to induce growth cone collapse and retraction. Proteins from somas or neurites were then specifically isolated as described in Experimental Procedures and Western blotted with phosphosite specific antibodies that recognize the phosphorylated activated form of ERK (P-ERK), or MEK (T218, T222, human sequence) or phosphoamino acids S298 and S292 of MEK, which modulate kinase activity in response to PAK and ERK kinase activity, respectively. Western blots of total cell ERK/MEK protein are shown for comparison.   B. Neurites were allowed to extend toward laminin for 18 hours (time 0) then induced to collapse with LPA for the indicated times and Western blotted for activated ERK-P and total ERK as described in A. C. Soma and neurite proteins were prepared as in A and Western blotted for the phosphorylated/activated form of Akt (p-Akt, S473) or total Akt protein. D. Cells were allowed to extend neurites for 18 hours (growth) and then stimulated with LPA to induce retraction. Rac and Cdc42 activation (Rac-GTP, Cdc42-GTP) were determined from isolated neurite and soma proteins using a GST-PBD pulldown assay and Western blot analyses. ERK served as loading

14

control. E. Cells were allowed to extend neurites to the lower surface for 8 hours (growth) and then stimulated with LPA for the indicated times. Somas and neurites were purified and Western blotted for the indicated proteins and/or specific phosphorylation sites. Crk Y221 phosphorylation is detected as a decrease in electrophoretic mobility in the gel. LASP-1 was first immunoprecipitated (IP) and then Western blotted with antiphosphotyrosine antibodies. Asterisk indicates the neurite/soma fold enrichment of the protein as determined by mass spectrometry and or Western blotting and densitometry. F. Cells were allowed to extend neurites to the lower surface for 8 hours (growth) and then stimulated with LPA for the indicated times. Somas and neurites were purified and Western blotted with anti-phosphotyrosine antibodies. Arrows show neurite specific proteins that decrease in response to LPA. Asterisk shows a neurite protein band that does not change in response to LPA. G. N1E-115 cells were either held in suspension (S) or allowed to attach (A) to laminin coated dishes for 45 minutes in the presence or absence of LPA and then Western blotted for activated ERK (p-ERK) or MEK S298 as in (A).

Fig. 5. Deactivation of ERK is necessary for LPA-induced N1E-115 neurite retraction. A**.** Quantification of neurite formation of NIE-115 cells either mock transfected or transfected with constructs encoding mutationally activated MEK (MEK-CA), or MEK-CA with S298 or S292 amino acids changed to alanine. Inset shows the level of MEK expression by Western blotting. B. Quantification of neurite formation for 6 hours in the presence of the MEK kinase inhibitor PD98059 (25 μm) or the vehicle DMSO (control). Inset shows the level of ERK phosphorylation and kinase activity by Western blotting as described in figure 4A. C. Cells were either mock transfected with a empty vector or transfected with HA tagged MEK-CA and allowed to extend neurites to the lower surface for 18 hours and then treated with or without LPA for 10 minutes to induce retraction and quantified as described in Figure 1D.   D. Somas and neurites were purified from cells transfected as in C and Western blotted with phosphospecific antibodies to activated p-ERK and MEK phosphorylated on S292 or S298. HA-MEK and total ERK Western blots are shown for comparison. E. Cells were allowed to extend neurites to the lower membrane surface for 12 hours then treated with the MEK inhibitor PD98059 for 60 minutes (time 0) before being treated with or without LPA for the indicated times. Neurites were quantified as in figure 1D.

Fig. 6. Inhibition of ROCK kinase activity prevents LPA-induce N1E-115 neurite retraction and prevents ERK inactivation. A. Neurites were allowed to extend to the lower surface of the membrane for 18 hours and then treated with or without the ROCK kinase inhibitor Y-27632 for 30 minutes prior to being stimulated with or without LPA for 10 minutes. Neurites were quantified as described in figure 1D. B. Neurites were isolated from cells treated as in A and Western blotted for activated ERK (p-ERK) or phosphorylated myosin light chain (p-MLC) on serine 19 or total MLC. C. Schematic model showing the possible signaling and phosphorylation mechanisms that mediate neurite extension and retraction in response to the collapsing factor LPA. Grey shaded circles with black text indicate the phosphorylation site and neurite growth/retraction ratio determined by mass spectrometry. Red text indicates fold change in protein abundance level between soma and neurite. A list of the depicted proteins and their associated regulatory molecules, and their neurite abundance and phosphorylation status are shown in sTable 3 (a) shows integrin mediated ERK activation and neurite extension pathway. (b) shows LPA induced neurite retraction pathway. Also see sFigure 1 for more details of the LPA/Rho pathway. (c) shows cytoskeleton-associated proteins that contain at least one phosphorylation site that conforms to the ERK amino acid consensus sequence Px(S)TP where x is any basic or neutral amino acid. Numbers in parentheses indicate the neurite growth/retraction ratio of the predicated ERK phosphorylation site as measured by mass spectrometry. CAS = p130CAS, Crk= C-CrkII, PKA = protein kinase A, FAK = focal adhesion kinase, MT = microtubules, MAPS = microtubule-associated proteins, ROCK = Rho kinase, Crmp-1 = collapsin response mediator protein 1.
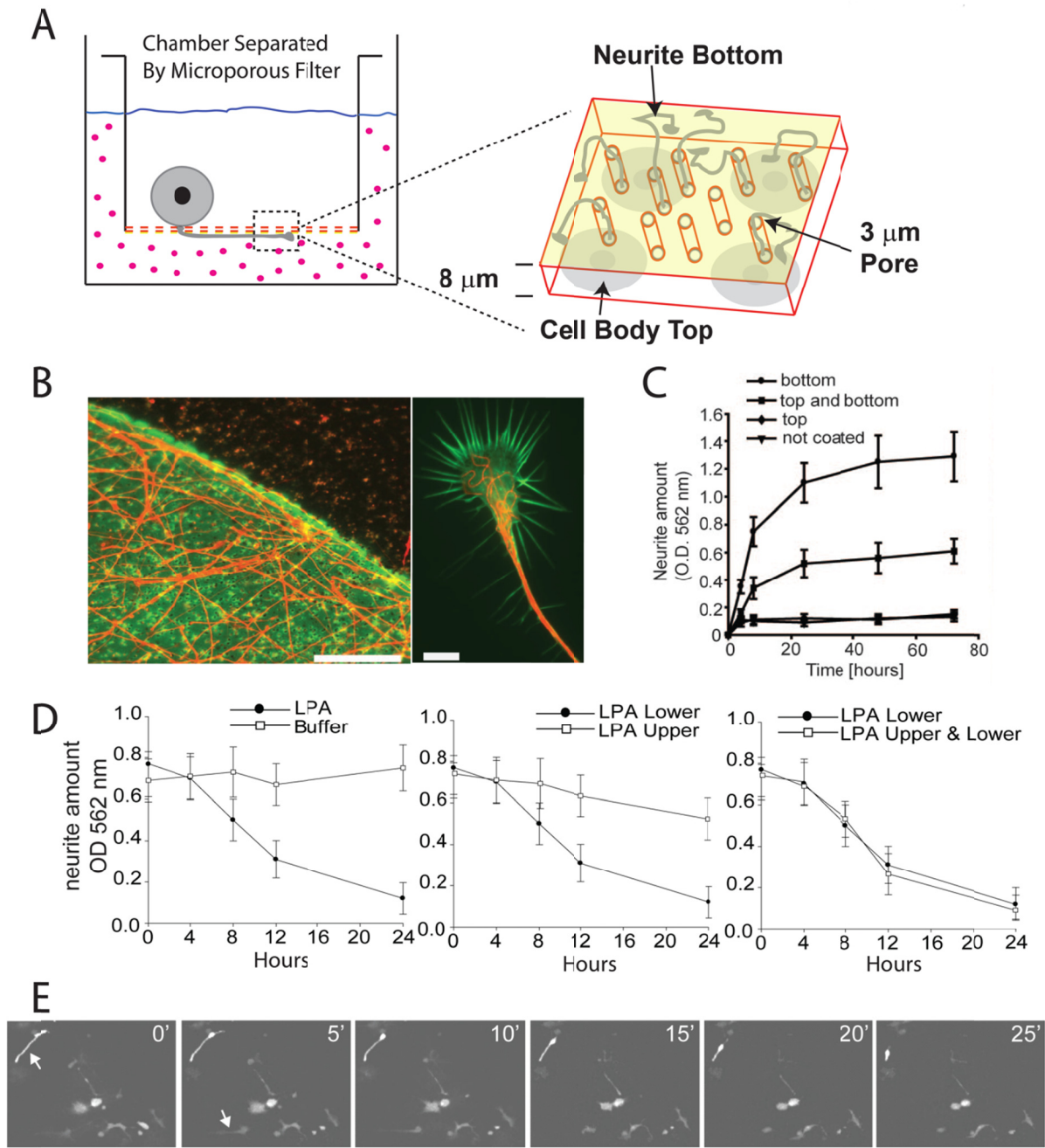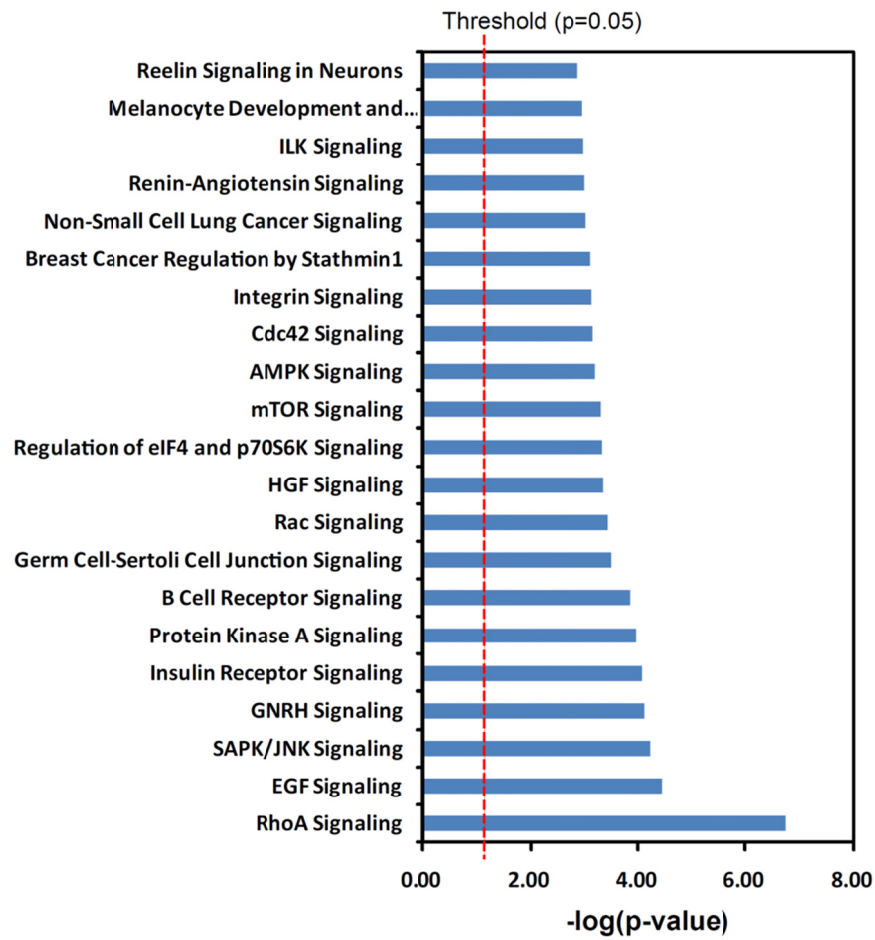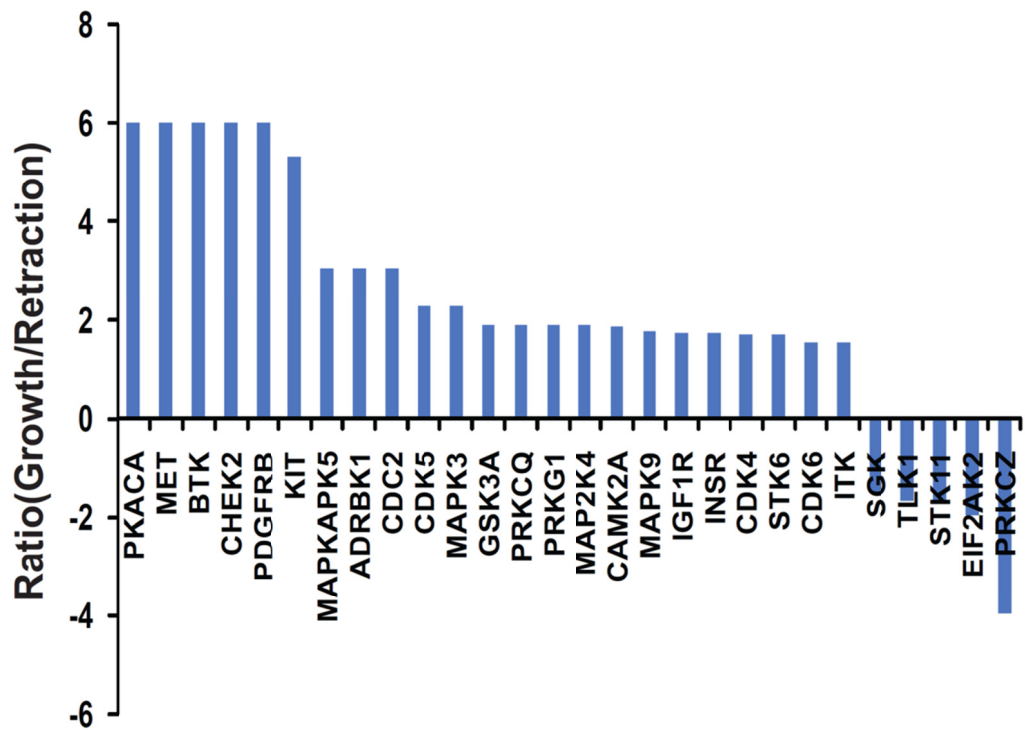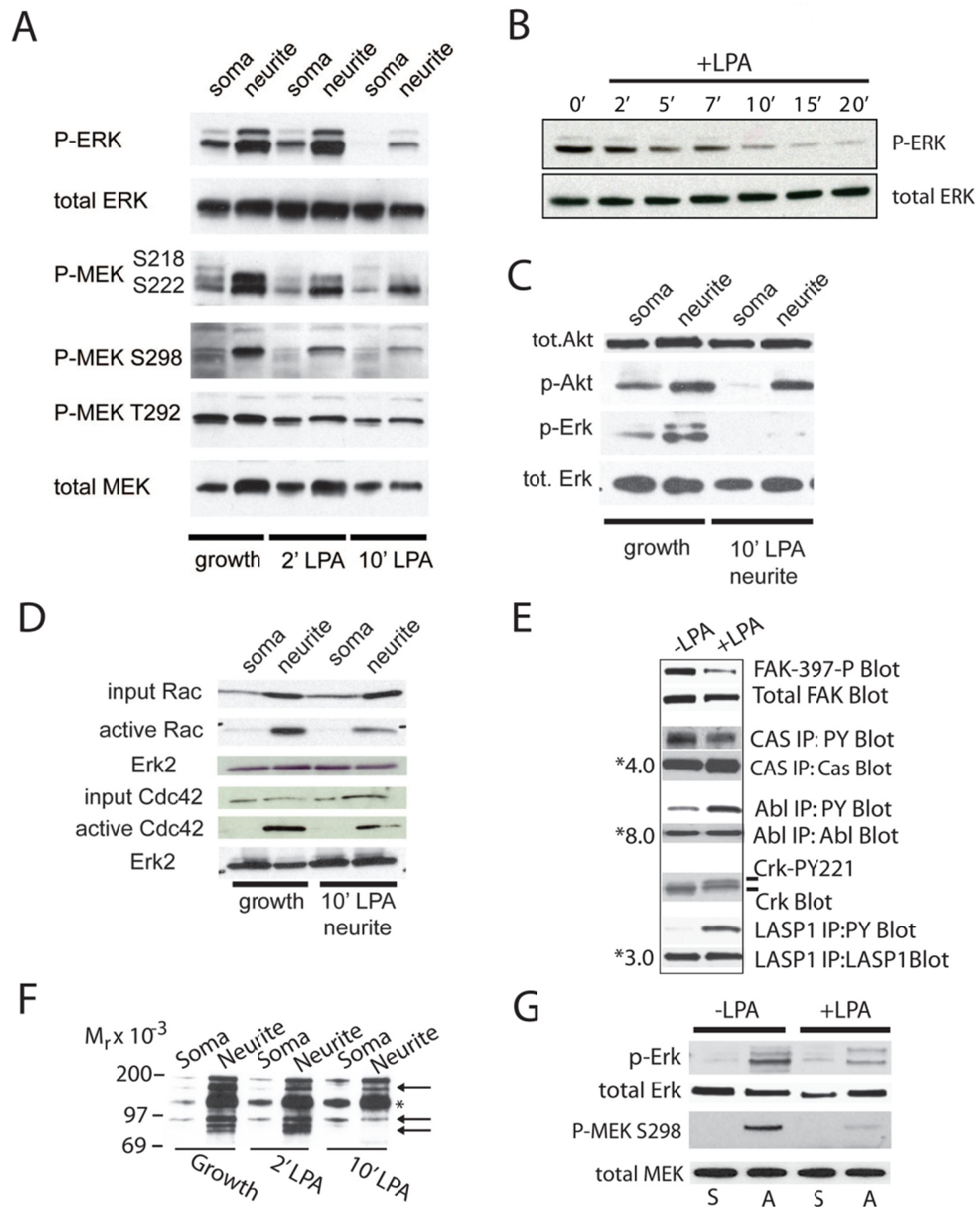
Fig. 1A-E

16

Fig. 2

Threshold (p=0.05)

Reelin Signaling in Neurons
Melanocyte Development and...
ILK Signaling
Renin-Angiotensin Signaling
Non-Small Cell Lung Cancer Signaling
Breast Cancer Regulation by Stathmin1
Integrin Signaling
Cdc42 Signaling
AMPK Signaling
mTOR Signaling
Regulation of eIF4 and p70S6K Signaling
HGF Signaling
Rac Signaling
Germ Cell-Sertoli Cell Junction Signaling
B Cell Receptor Signaling
Protein Kinase A Signaling
Insulin Receptor Signaling
GNRH Signaling
SAPK/JNK Signaling
EGF Signaling
RhoA Signaling

0.00   2.00   4.00   6.00   8.00

-log(p-value)

Fig. 3

18

Fig. 4A-G

Fig. 5A-E

A MEK Blot

Neurites (O.D. 562 nm)

Mock MEK-CA MEK-CA-S298A MEK-CA-S292A

B Neurites (O.D. 562 nm)

Control PD

P-ERK

total ERK

Control PD98059

C MOCK MEK-CA

Neurites (O.D. 562 nm)

LPA - + - +

D

growth LPA 10' growth LPA 10'

soma neurite soma neurite soma neurite soma neurite

P-ERK

total ERK

HA-Blot

P-MEK S298

P-MEK S292

MOCK CA MEK

E 0' 2.5' 5' 10'

Neurites (O.D. 562 nm)

LPA - - + + + + + +
PD98059 - + - + - + - +

20

Fig. 6A-C

A

B

C